2024 Tenth Indian Control Conference (ICC)
9 - 11 December, 2024
IISER Bhopal, India

Morse Potential Field based Guided Exploration using an Augmented Directed Network

Amritesh Maitra and Debasish Ghose

Abstract— **This paper explores Morse Potential based Attraction-Repulsion (MPAR) methodology in a modified cyclic pursuit framework to achieve swarm aggregation leading to circumnavigation behaviour. However, MPAR, being a nonlinear range-dependent function, displays complex drifting behavior and arbitrary shape of the swarm. This complexity is sensitive to the initial conditions of the agents and appears to be analytically intractable, thus making it unusable in many applications. We address this issue by making one of the agents stationary and modifying the cyclic network. It is shown that circumnavigation is achieved with the target information available to only one agent. Furthermore, based on the initial velocity perturbation of a follower agent, some non-intuitive aggregation patterns emerge. We use a LOS-based analysis framework to explain these patterns, which can be used for location-sensitive applications and for search and exploration.**

Keywords: Morse potential, Potential-based aggregation, Swarm systems, Aggregation behavior, Directed networks

I. Introduction

This paper presents some analysis and results of a Morse Potential based Attraction-Repulsion (MPAR) methodology applied to a directed network similar to cyclic pursuit but with some important distinctions, with the objective of achieving certain exploratory behaviour of the agent swarm such as circumnavigation. Circumnavigation about a target, or coordinated standoff circle tracking, using multiagent systems (MAS) has numerous potential applications like surveillance, convoy protection, forest fire mitigation, coordinated transport, satellite coverage maintenance, etc., and has gained considerable attention from the guidance and control community over the last two decades. Linear cyclic pursuit has been shown to achieve positional consensus, where agents converge to a single point [1]–[4]. Nonlinear cyclic pursuit and generalizations of the basic cyclic pursuit paradigm has also attracted considerable attention [5]–[8]. Some applications of a swarm of agents is to explore areas of interest and also achieve coordinated stand-off tracking of designated targets [9]–[18]. The basic cyclic pursuit paradigm is not useful for such applications as it is more tuned toward positional consensus.

In this paper, we consider a guided exploration problem using a non-linear cyclic pursuit paradigm in which the Morse potential field defines the forces between a leader and its follower. Morse potential-based attraction-repulsion (MPAR) in a swarm system has the benefit of ensuring coherent steady configurations within a given range of parameters [19], [20]. MPAR has attracted the attention of researchers for its potential use in large-scale swarms [21], [22], [23] due to its dependence only on inter-agent distances. The practicability of MPAR in realistic swarm systems under communication constraints has been explored in [24] for decentralized swarm control. It has been shown that coherent configurations are possible even under extremely sparse communication when one swarm member is randomly connected to 1 or 2 other member(s) in a decentralized control setting over a directed network, even if the underlying network is not explicitly of a special nature (that is, balanced, signed, circulant, rigid, presence of a direct spanning tree, etc.).

Motivated by these observations, we consider the Morse potential-based attraction-repulsion (MPAR) as a candidate control law for nonlinear cyclic pursuit, which combines the extensive application areas of cyclic pursuit and of MPAR as a potential paradigm for simple decentralized control. However, our work shows that a simplistic application of MPAR in the cyclic pursuit scenario leads to drift in the swarm and its centroid, whose behavior is difficult to establish analytically. Given this, carrying out any exploration tasks using this paradigm is difficult, especially when the exploration areas are pre-designated.

With this in mind, our work proposes a paradigm in which a subset of the agents in the swarm is made stationary so that exploration is confined to the areas near these stationary agents. Although this seems to be an obvious solution, we show that the resulting swarm behavior is non-intuitive because the exploration areas are defined not just by the location of the stationary agent but also by its immediate followers. We also show that a circumnavigation functionality for the swarm can be created by introducing perturbations to the immediate follower of the stationary agents. In this paper we present the study related to a single stationary agent.

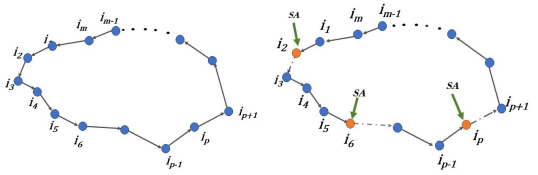
II. Preliminaries

A. Cyclic Network and Augmented Network

Figure 1(a) shows a generalized cyclic network of m agents i_1, i_2, …, i_m, in which a general agent i_p tracks (or follows) its leading agent i_{p+1} and is subsequently tracked by agent i_{p-1}. In Fig. 1(b), the cyclic network shown in Fig. 1(a) is augmented with q number of *stationary agents (SAs)*. A *SA* in the context of this paper is defined as an agent whose link to its leader is ineffective. Hence, it would remain stationary as it does not receive a tracking command or external stimulus. However, it would continue to be tracked

Amritesh Maitra is a PhD student in the Department of Aerospace Engineering at the Indian Institute of Science, Bangalore 560012, India. amriteshm@iisc.ac.in

Debasish Ghose is a professor in RBCCPS and the Department of Aerospace Engineering at the Indian Institute of Science, Bangalore 560012, India. dghose@iisc.ac.in



(a) (b)

Fig. 1: (a) A generalized cyclic network and (b) A directed network augmented from (a) for guided exploration. SA indicates Stationary Agents (in orange).

by its trailing agent, or follower, in the original (cyclic) network. It is evident that a cyclic network augmented with q *SAs* will be an ensemble of q linear directed links, and will no longer be cyclic in the original sense. For the remainder of the paper, a network (cyclic or otherwise) containing one or more *SAs* will be called an Augmented Directed Network. The idea of using one or more SA's is to concentrate the exploration or circumnavigation behavior of a subset of the swarm of agents to the approximate vicinity of the SA.

The agent indexing in Fig. 1 has been made sequentially for ease in understanding without any loss in generalization. Also, the arrows indicating edge direction in figure 1 denote the direction of agent movement along the link (that is, a connectivity graph). If we visualize an in-degree information graph, the corresponding edge direction will be reversed, as agent i_p obtains information from agent i_{p+1}.

B. Morse Potential-based Attraction-Repulsion (MPAR)

Let i be a member of an MAS or a swarm. A generalized Morse Potential field for the agent i, defined for all-to-all communication is given by [19], [20]:

$$\begin{aligned} U_i &= \sum_{i\neq j}\left[C_r e^{-\left(\frac{\|X_i-X_j\|}{l_r}\right)} - C_a e^{-\left(\frac{\|X_i-X_j\|}{l_a}\right)}\right] \\ &= \sum_{i\neq j}\left[C_r e^{-\left(\frac{r_{ij}}{l_r}\right)} - C_a e^{-\left(\frac{r_{ij}}{l_a}\right)}\right] = U(r_{ij}) \end{aligned} \tag{1}$$

Here, l_a and l_r are attraction and repulsion ranges, and C_a and C_r are coefficients of attraction and repulsion. The ratios $C = C_r/C_a$ and $l = l_r/l_a$ are design parameters chosen to ensure a desirable steady state milling or circumnavigation under an ideal all-to-all communication.

The resultant force on any agent is the negative divergence of the potential mentioned above, that is,

$$\begin{aligned} F(r_{ij}) = -\nabla_{i\neq j}U(r_{ij}) = \sum_{i\neq j}\Big[&(C_r/l_r)\, e^{-\|X_i-X_j\|/l_r} \\ &- (C_a/l_a)\, e^{-\|X_i-X_j\|/l_a}\Big] \end{aligned} \tag{2}$$

Let us assume a neighborhood $\mathcal{N}_i$ is defined for agent i, which is not all-to-all (as assumed in the original formulation). The corresponding Morse potential and the resultant force are modified accordingly and the equations of motion for agent i acting under MPAR becomes

$$\begin{aligned} \dot{X}_i &= V_i \\ \dot{V}_i &= \left(\alpha - \beta\left\|V_i^2\right\|\right) V_i - \frac{1}{|\mathcal{N}_i|}\sum_{j\in\mathcal{N}_i}\nabla_{x_i} U\left(\|X_i - X_j)\|\right) \end{aligned} \tag{3}$$

where $|\mathcal{N}_i|$ is the number of agents in the neighborhood of agent i; $\nabla(\cdot)$ is gradient of a scalar quantity; and $\|X_i - X_j\|$ is the Euclidean distance between agents i and j. In particular, for m agents, $\mathcal{N}_i = i+1,\ i = 1\ldots m-1$; and $\mathcal{N}_m = 1$ for a cyclic network and $\mathcal{N}_m = \emptyset$ for a directed tree network. In (3), α and β are the self-propelling and friction terms, respectively, whose significance can be found in [19].

C. Drifting Behavior of Cyclic Pursuit under MPAR

In a linear cyclic pursuit case, the positional consensus always occurs at the weighted centroid of the initial agent positions [3], [4], irrespective of the cyclic connection topology. In this subsection, we show that this is not the case when MPAR is used as the force model in the cyclic pursuit paradigm, and each cyclic connection pattern will lead to a different exploration area.

Fig. 2 shows the evolution of cyclic pursuit for three equivalent swarms deployed within a space of $100\mathrm{m}\times 100\mathrm{m}$. The agents occupy the same initial locations in all three swarms, but their cyclic connectivities are different. Initial velocities of agents in all the three cases are zero. We observe that under the current nonlinear version of cyclic pursuit with MPAR, convergence at the weighted centroid does not happen. Moreover, the drifting of the centroid, even without any initial velocities, is not useful for exploration tasks, as it is difficult to establish the direction of this drift with the chosen parameters. Hence, the effect of different cyclic connection patterns cannot be used to determine the exploration region. As there are $m!$ different cyclic connections possible, and each of them can lead to different areas of exploration, evaluating them (especially with different possible weights in the MPAR model) would be prohibitively expensive in terms of computations.

III. Analysis with a Single Stationary Agent

Consider that one of the agents, say T, is stationary, which implies that $V_T = 0$ irrespective of the position of its leader. Note that when we make agent T stationary, the cyclic pursuit system becomes a linear pursuit system with T as the stationary leader agent followed by a directed tree link with a topology as depicted in Fig. 1(b) with the link between T and $T+1$ missing. In this section, we study the kinematics of a system comprising angle stationary agent and a subsequent follower agent. See Fig. 3(a), where X_i and X_T indicate position vectors of the agents i and T. The relative velocity vector X_{iT} denotes the vector from agent i and T, and is given by $X_{iT} = X_T - X_i$. All the vectors are defined with respect to the origin $(0,0)$ of an inertial coordinate system. The follower agent i is attracted to a leader T under MPAR, with the LOS length and angle between them being R and θ. The LOS equations with $V_T = 0$ are as follows,

$$\dot{R} = -V_i\cos(\psi_i - \theta);\quad R\dot{\theta} = -V_i\sin(\psi_i - \theta) \tag{4}$$

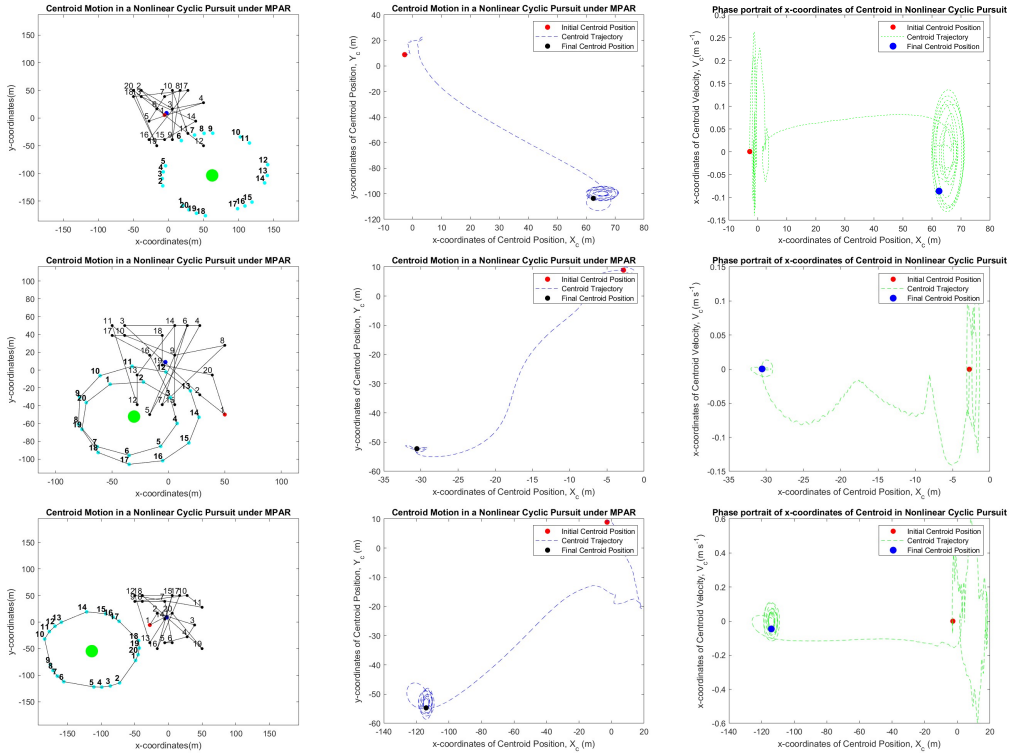
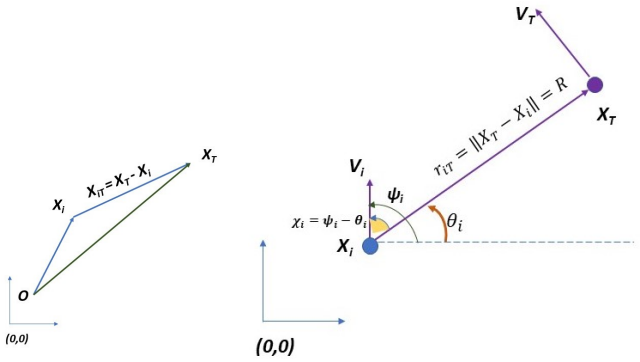


Fig. 2: Evolution of three swarms with same initial locations, but different cyclic connectivity over 5000 seconds. The first column shows the initial (black dots) and final (Indigo colored dots) configurations of a 20-agent swarm. The blue dot and green dots indicate the location of centroids at the beginning and end, respectively. The second column shows the motion of the centroids for the three equivalent swarms. The third column shows the phase portrait of the x-coordinates of the centroid.



(a) (b)

Fig. 3: (a) LOS vector convention (b) Initial engagement

Here, ψ_i is the heading angle of agent i. The MPAR force between i and j is

$$F(r_{ij}) = \left[(C_r/l_r)e^{-r_{ij}/l_r} - (C_a/l_a)e^{-r_{ij}/l_a}\right] = F(R) \quad (5)$$

From Fig. 3(b), the force component $\left(\alpha - \beta \left\|V_i^2\right\|\right) V_i$ is directed along V_i, and so does a component of F_R resolved along the heading of agent i (that is, V_i).

The equations for V_i is obtained from (3) for a linear topology with single agent interaction as,

$$\dot{V}_i = \left(\alpha - \beta \left\|V_i^2\right\|\right) V_i + F(R)\cos\chi_i \quad (6)$$

Resolving the acceleration along $x-$ and $y-$ directions,

$$\dot{V}_{xi} = \left(\alpha - \beta \left\|V_i^2\right\|\right) V_i \cos\psi_i + F(R)\cos\theta \quad (7)$$

$$\dot{V}_{yi} = \left(\alpha - \beta \left\|V_i^2\right\|\right) V_i \sin\psi_i + F(R)\sin\theta \quad (8)$$

We define the heading of agent i with respect to the LOS as $\chi_i = \psi_i - \theta$, where $\psi_i = \tan^{-1}\left(V_{y_i}/V_{x_i}\right)$. Then,

$$\dot{\chi}_i = \dot{\psi}_i - \dot{\theta} \quad (9)$$

The rate of agent heading change ($\dot{\psi}_i$) is obtained as,

$$\dot{\psi}_i = \frac{d}{dt}\tan^{-1}\left(\frac{V_{y_i}}{V_{x_i}}\right) = -\frac{F(R)}{V_i}\sin\left(\psi_i - \theta\right) \quad (10)$$

Substituting (10) and (4) in (9), we get,

$$\begin{aligned}\dot{\chi}_i &= \dot{\psi}_i - \dot{\theta} = -\frac{F(R)}{V_i}\sin(\psi_i - \theta) + \frac{V_i}{R_i}\sin(\psi_i - \theta) \\ &= \left[(-F(R)/V_i) + V_i/R\right]\sin\chi_i \quad (11)\end{aligned}$$

In compact form, the trajectory of the LOS between the *SA* and follower is given by,

$$\begin{bmatrix}\dot{R} \\ \dot{\chi}_i \\ \dot{V}_i\end{bmatrix} = \begin{bmatrix}-V_i\cos\chi_i \\ \left(\frac{V_i}{R} - \frac{F(R)}{V_i}\right)\sin\chi_i \\ \left(\alpha - \beta\left\|V_i^2\right\|\right)V_i + F(R)\cos\chi_i\end{bmatrix} \quad (12)$$

At steady state,

$$\begin{bmatrix}\dot{R} & \dot{\chi} & \dot{V}_i\end{bmatrix}^T = 0 \quad (13)$$

with the corresponding values $R = R_0, V_i = V_{i0}, \chi_i = \chi_{i0}$

(note that the subscript '0' here refers to the steady state values and not to the initial conditions).

Remark 1. The first row in (12) achieves equilibrium for $V_i = 0$ or $\cos\chi_{i0} = 0$. However, for circumnavigation, $V_{i0} \neq 0$. Thus, $\chi_{i0} = (2n+1)(\pi/2)$, where $n = 0, \pm1, \pm2, \ldots$.

Remark 2. If $\chi_i = 0$ at $t = 0$, then $\sin\chi_i = 0$ and $\dot{\chi}_i = 0$ throughout and no LOS angle variation happens. We call this as the unperturbed initial velocity case. A nonzero $\cos\chi_i$ component ensures $\dot{R}$ also remains undamped. This leads to sustained oscillation along the LOS between the stationary agent and the follower agent. When $\chi_i \neq 0$, we have $\sin\chi_i \neq 0$. This will lead to circumnavigation behavior. We will call this the perturbed initial velocity case. We will demonstrate both these phenomena in the simulations.

Remark 3. Note that for a multiagent neighborhood setting, in (3), $\dot{V}_i$ is obtained as a vector sum of all the interaction due to all the neighbors, while in the current problem setting, the $\dot{V}_i$ component has been derived analytically from exact agent-agent LOS kinematics for a directed linear network. The directionality of the *SA*-follower network manifests in the expression through the contribution of $\cos\chi_i$ term. In the rest of the paper, we will use (6) for the acceleration component of agent i.

For the unperturbed case (see Remark 2) we have the following proposition on a linearized analysis of the system behavior at the equilibrium point. A word of caution, that the lineraized stability analysis does not completely reveal the nature of the behavior of the system states at the equilibrium point, is in order. Some indications of an approach to stability analysis of this system can be found in [25].

Proposition 1. *In the unperturbed case, an agent i following a stationary agent (SA) under MPAR interaction, in the linearized form, displays unstable behavior when the initial heading of i with respect to the LOS is zero.*

Proof. We have $\chi_i = 0$, $\sin\chi_i = 0$, and $\cos\chi_i = 1$. Hence, (12) reduces to,

$$\begin{bmatrix}\dot{R}\\ \dot{V}_i\end{bmatrix} = \begin{bmatrix}-V_i\\ \left(\alpha - \beta\left\|V_i^2\right\|\right)V_i + F(R)\end{bmatrix} \tag{14}$$

It can be observed that $\dot{R} = 0$ when $V_i = 0$. Thus, $\left(\alpha - \beta\left\|V_i^2\right\|\right)V_i = 0$, and so $F(R) = 0$ at $R = R_0$. Hence, equating the attractive and repulsive components of (5) with $r_{ij} = R_0$, we get,

$$r_0 = \frac{1}{(1/l_r - 1/l_a)}\ln\left(\frac{C_r}{C_l}\frac{l_a}{l_r}\right) = \frac{1}{(1/l_r - 1/l_a)}\ln\left(\frac{C}{l}\right) \tag{15}$$

Let $\overline{F}(R)$ be the derivative of $F(R)$ with respect to R. The linearized form of the reduced LOS kinematics is,

$$\begin{bmatrix}\dot{R}\\ \dot{V}_i\end{bmatrix} = \begin{bmatrix}0 & -1\\ \overline{F}(R) & \alpha\end{bmatrix}\begin{bmatrix}R\\ V_i\end{bmatrix} \tag{16}$$

where

$$\overline{F}(R) = -\frac{C_r}{l_r^2}e^{-\frac{r_{ij}}{l_r}} + \frac{C_a}{l_a^2}e^{-\frac{r_{ij}}{l_a}} \tag{17}$$

The eigenvalues of the linearized equation (16) is given by

$$\lambda = \left(\alpha \pm \sqrt{\alpha^2 - 4\overline{F}(R)}\right)/2 \tag{18}$$

Since $\alpha > 0$, the equilibrium point is unstable. □

Consider an example, where $C_a = 20$, $C_r = 50$, $l_a = 100$, $l_r = 2$,$\alpha = 0.07$, $\beta = 0.05$, we obtain, $r_0 = 9.8537$m. So, $[9.8537, 0]$ is a potential equilibrium point. The eigenvalues from (18) are, $\lambda = 0.035 \pm 0.18006$. However, note that the above analysis is based on the linearized form of the equations. An analysis of the non-linear equations will reveal more reliable behavior around the equilibrium point, but is beyond the scope of this paper.

Proposition 2. *Define* $\overline{F}(R_0) + \alpha/(\beta R_0^2) = M(\alpha, \beta, C_r, C_a, l_r, l_a, R_0) = M$ *where* $\overline{F}(R_0)$ *is obtained from (17). Appropriate Morse parameter choices will ensure steady-state circumnavigation for a system comprising a Stationary Agent (SA) and a single follower for a perturbed initial velocity case (Remark 2).*

Proof. For rotational equilibrium corresponding to (12), one potential equilibrium point is $\chi_{i0} = \pi/2$, $V_{i0} = \sqrt{\alpha/\beta}$, and an equilibrium value of R_0, such that $F(R_0) = V_{i0}^2/R_0$, thereby setting (12) to zero. Evaluating the Jacobian matrix at the equilibrium point, that is, $R = R_0$, $V = V_{i0}$, $\chi_{i0} = \pi/2$, the resultant characteristic equation can be obtained. Analyzing the characteristic equation will yield analytical expressions for the conditions of stability. We omit the details due to space constraints. The resultant equation characteristic equation is,

$$\begin{aligned}\lambda^3 + 2\alpha\lambda^2 + \lambda\{2F(R_0)/R_0 + \overline{F}(R_0) + \alpha/(\beta R_0^2)\}\\ +2\alpha\{\overline{F}(R_0) + \alpha/(\beta R_0^2)\} = 0\end{aligned} \tag{19}$$

Substituting, $\overline{F}(R_0) + \alpha/(\beta R_0^2) = M(\alpha, \beta, C_r, C_a, l_r, l_a, R_0) = M$ in (19),

$$\lambda^3 + 2\alpha\lambda^2 + \lambda\{2F(R_0)/R_0 + M\} + 2\alpha M = 0 \tag{20}$$

The stability conditions are obtained as: $\alpha > 0$, $2F(R_0)/R_0 > 0$, and $M > 0$. The first two inequalities are automatically satisfied, and the third one $M > 0$ can be ensured by appropriate choice of Morse parameters. Details are omitted in the current paper. This shows that circumnavigation for the perturbed case can be achieved by proper choice of the Morse parameters. □

The above analysis shows that the perturbed case may lead to smoother circumnavigation behavior in the vicinity of the stationary agent while the swarm's behavior in the unperturbed case will be affected by the instability of the equilibrium point.

IV. Simulation Results

In Figures 4 and 5, representative behaviors of a $9-$ agent network with 1 stationary agent (SA) have been shown. Fig 4a shows the initial configuration with agent 9 as the *SA* and agent 8 as the immediate follower connected to the *SA*. The first scenario (Fig. 4) is the unperturbed case and the second scenario (Fig. 5) is the perturbed case where a

nominal perturbation, normal to the LOS between the *SA* and its follower, is provided to agent 8. In both cases, the linked agent group is initially dispersed within a 100m $\times$ 100m square. In both cases, the parameters have the values $C_a = 20$, $C_r = 50$, $l_a = 100$, $l_r = 2$,$\alpha = 0.07$, $\beta = 0.05$.

A. Unperturbed Initial Velocity Case

See Fig.4. In the absence of any perturbation, agent 8's motion is always along the LOS with the *SA*. Note that agent 7 lies on the same straight line as the *SA* and agent 8 and also has motion along its LOS with agent 8. Hence, both agents 7 and 8 have oscillatory trajectories as seen in Figs. 4d and 4f. It is observed that the configuration after 1000s does not attain a stable configuration but rather forms an oscillatory agent ensemble, as evident from the velocity plots in Figs. 4e and 4f. From agent 6 onwards, the non-zero heading angles will result in damped oscillatory trajectories.

The following are the notable features of the overall aggregation phenomenon:

1) From the velocity plots Fig. 4e and Fig. 4f, we observe agent 1, the one farthest from the *SA*, tends to attain a constant speed after some intermediate non-smooth motions. From agent 6 to agent 1, as we move along the directed link away from the *SA*, the velocity profile tends to be smoother. Hence, we can qualitatively state that the effect of the instability in the absence of perturbation tends to get damped as we move away from the stationary agent.
2) From Fig. 4b, we see that the centroid tends to be in a region somewhat away from the *SA*, and the swarm displays exploratory behavior in that region. This region is approximately centered around the mean position of agent 7. From this observation, we can say that the center of the exploration region is determined by the mean position of the linearly oscillating agent that is farthest from the *SA*. So, by using a suitable placement of the oscillating follower agents (in this case, agents 7 and 8), the location of the exploration region can be designed. The radius of the approximate circle within which agents move along different oscillatory trajectories is determined by the Morse parameters. This opens up a possible scheme for an exhaustive guided search and exploration mission of a desired region.

B. Perturbed Initial Velocity Case

Fig. 5 shows the plots for the case when agent 8 is perturbed by a nominal velocity normal to its LOS with the *SA*. The following are the notable observations from the simulation results.

1) Agent 8, connected directly to the *SA*, has a steady-state stand-off radius slightly less than the rest.
2) The steady state agent velocities for the agents are different. But in the steady-state, the agents have almost uniform angular velocities and circumnavigate about the *SA*. As agents move in circles of different radii, the velocities may differ.

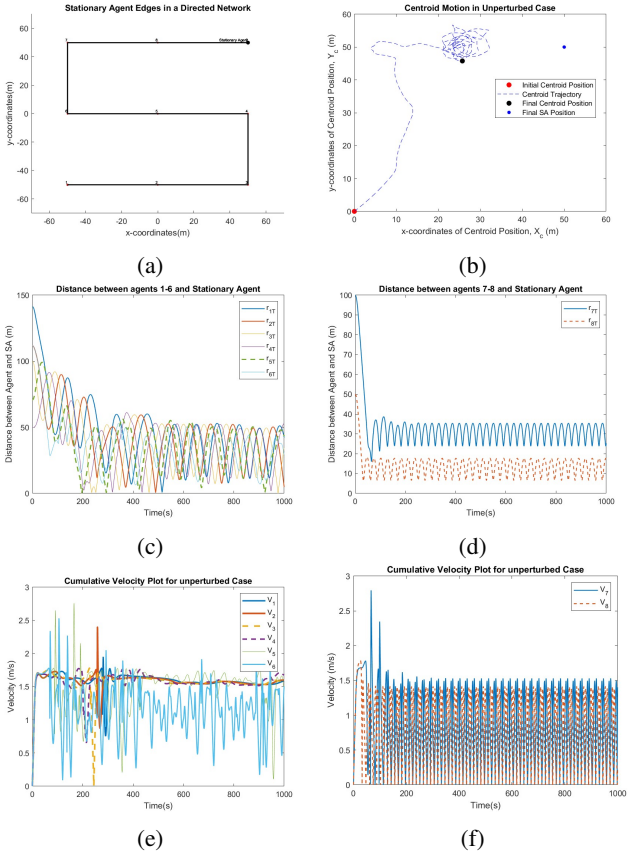


Fig. 4: A 9$-$ agent unperturbed initial velocity case (a) Initial deployment (b) Centroid trajectory $0 - 1000$s (c) Distances between *SA* and agents $1 - 6$ (d) Distances between *SA* and agents $7 - 8$ (e) Velocities of agents $1 - 6$ (f) Velocities of agents 7 and 8

3) The steady-state agent locations along the stand-off circle are not spatially sequential as in the original link
4) Agent 8, under perturbation achieves circumnavigation first among the linked agents. As we move down the link from agents 7 to 1, the expected time for achieving circumnavigation increases.
5) When we apply MPAR in a directed link in presence of *SA*, we can achieve an almost perfect circumnavigation, the "imperfection" stemming from the observation that the agent connected to *SA* rotates at a radius slightly different from the others.
6) In 5a, it can be seen that the steady state centroid coincides with the location of the *SA* and is non-oscillatory after circumnavigation is achieved. Hence, the perturbed case can be used for circumnavigation around specific target points.

Although the above set of simulations has been done for 9 agents, the results have been verified for a higher number of agents as well.

V. Conclusion

In this paper we have analyzed how a multiagent system or a swarm might behave under MPAR-based interactions

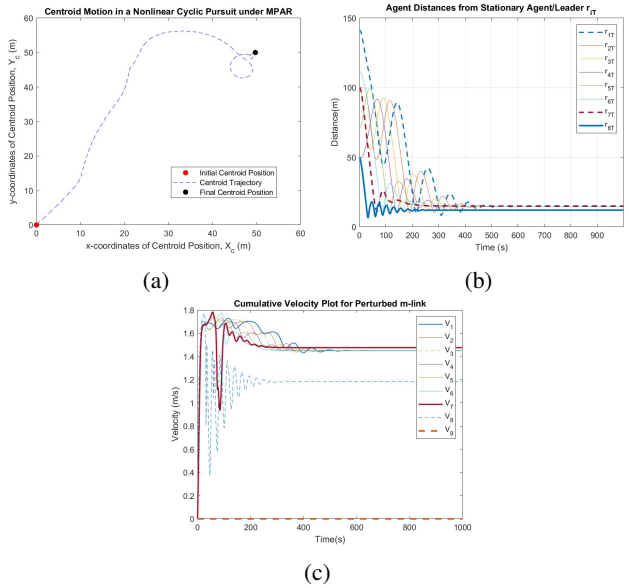


Fig. 5: A $9-$ agent perturbed initial velocity case (a) Centroid trajectory $0-1000$s (b) Variation of agent-SA distance r_{iT} (c) Agent velocities

connected via a linear, directed graph. By considering the notion of a stationary agent (SA), two distinct classes of behaviors have been characterized, based on presence or absence of a perturbation. The zero perturbation case can be used to achieve exploration tasks by the swarm members connected through a directed link. Through the perturbed case, we have achieved a stable rotating configuration. This establishes that over a minimally connected network, MPAR can be used for circumnavigation. This is an improvement over the requirement of an all-to-all communication network for achieving milling (a phenomenon of identical functionality), as originally proposed in [19]. As expected, in coupled nonlinear systems, the effect of initial conditions in a swarm acting under MPAR is not straightforward and hence the final location of the stable configuration is analytically intractable without an explicit control scheme. In the current paper, the paradigm of adding a *stationary agent* within a network has been exploited to achieve directed exploration and circumnavigation about a target by implicit control itself, that is, solely by choice of coefficients (Morse parameters). Future research will focus on the analytical development of network behaviors under MPAR in the presence of single and multiple *SAs*. A thorough understanding of the connection of Morse parameter choices and steady-state properties of the network will help us in mission planning, especially for decentralized control of multiagent, multitarget missions.

REFERENCES

[1] Z. Lin, M. Broucke, and B. Francis, "Local control strategies for groups of mobile autonomous agents," *IEEE Transactions on automatic control*, vol. 49, no. 4, pp. 622–629, 2004.

[2] J. A. Marshall, M. E. Broucke, and B. A. Francis, "Formations of vehicles in cyclic pursuit," *IEEE Transactions on automatic control*, vol. 49, no. 11, pp. 1963–1974, 2004.

[3] ——, "Pursuit formations of unicycles," *Automatica*, vol. 42, no. 1, pp. 3–12, 2006.

[4] A. Sinha and D. Ghose, "Generalization of linear cyclic pursuit with application to rendezvous of multiple autonomous agents," *IEEE Transactions on Automatic Control*, vol. 51, no. 11, pp. 1819–1824, 2006.

[5] ——, "Generalization of nonlinear cyclic pursuit," *Automatica*, vol. 43, no. 11, pp. 1954–1960, 2007.

[6] D. Mukherjee and D. Ghose, "Generalized hierarchical cyclic pursuit," *Automatica*, vol. 71, pp. 318–323, 2016.

[7] J.-C. Juang, "On the formation patterns under generalized cyclic pursuit," *IEEE Transactions on Automatic Control*, vol. 58, no. 9, pp. 2401–2405, 2013.

[8] L. Ma and N. Hovakimyan, "Vision-based cyclic pursuit for cooperative target tracking," *Journal of Guidance, Control, and Dynamics*, vol. 36, no. 2, pp. 617–622, 2013.

[9] E. W. Frew, D. A. Lawrence, and S. Morris, "Coordinated standoff tracking of moving targets using lyapunov guidance vector fields," *Journal of guidance, control, and dynamics*, vol. 31, no. 2, pp. 290–306, 2008.

[10] T. H. Summers, M. R. Akella, and M. J. Mears, "Coordinated standoff tracking of moving targets: Control laws and information architectures," *Journal of Guidance, Control, and Dynamics*, vol. 32, no. 1, pp. 56–69, 2009.

[11] A. A. Pothen and A. Ratnoo, "Curvature-constrained lyapunov vector field for standoff target tracking," *Journal of Guidance, Control, and Dynamics*, vol. 40, no. 10, pp. 2729–2736, 2017.

[12] A. Jain and D. Ghose, "Collective circular motion in synchronized and balanced formations with second-order rotational dynamics," *Communications in Nonlinear Science and Numerical Simulation*, vol. 54, pp. 156–173, 2018.

[13] ——, "Synchronization of multi-agent systems with heterogeneous controllers," *Nonlinear Dynamics*, vol. 89, pp. 1433–1451, 2017.

[14] A. Jain, D. Ghose, and P. P. Menon, "Multi-vehicle formation in a controllable force field with non-identical controller gains," *IET Control Theory & Applications*, vol. 12, no. 6, pp. 802–811, 2018.

[15] A. Sen, S. R. Sahoo, and M. Kothari, "Cooperative target-centric formation control without relative velocity measurements under heterogeneous networks," *Journal of Intelligent & Robotic Systems*, vol. 87, pp. 683–698, 2017.

[16] ——, "Circumnavigation on multiple circles around a nonstationary target with desired angular spacing," *IEEE Transactions on Cybernetics*, vol. 51, no. 1, pp. 222–232, 2019.

[17] ——, "Containment using incomplete agent information over a digraph," *IEEE Control Systems Letters*, vol. 4, no. 3, pp. 614–619, 2020.

[18] D. Li, G. Ma, W. He, S. S. Ge, and T. H. Lee, "Cooperative circumnavigation control of networked microsatellites," *IEEE Transactions on Cybernetics*, vol. 50, no. 10, pp. 4550–4555, 2019.

[19] M. R. D'Orsogna, Y.-L. Chuang, A. L. Bertozzi, and L. S. Chayes, "Self-propelled particles with soft-core interactions: patterns, stability, and collapse," *Physical review letters*, vol. 96, no. 10, p. 104302, 2006.

[20] Y.-L. Chuang, M. R. D'orsogna, D. Marthaler, A. L. Bertozzi, and L. S. Chayes, "State transitions and the continuum limit for a 2d interacting, self-propelled particle system," *Physica D: Nonlinear Phenomena*, vol. 232, no. 1, pp. 33–47, 2007.

[21] J. Hindes, V. Edwards, S. Kamimoto, G. Stantchev, and I. B. Schwartz, "Stability of milling patterns in self-propelled swarms on surfaces," *Physical Review E*, vol. 102, no. 2, p. 022212, 2020.

[22] J. Hindes, V. Edwards, K. S. Kasraie, G. Stantchev, and I. B. Schwartz, "Swarm shedding in networks of self-propelled agents," *Scientific Reports*, vol. 11, no. 1, p. 13544, 2021.

[23] J. Hindes, V. Edwards, M. A. Hsieh, and I. B. Schwartz, "Critical transition for colliding swarms," *Physical Review E*, vol. 103, no. 6, p. 062602, 2021.

[24] A. Maitra and D. Ghose, "Aggregation in multi-agent systems under connectivity constraints in a potential-based system," in *International Conference on Sustainable and Innovative Solutions for Current Challenges in Engineering & Technology*. Springer, 2023, pp. 295–310.

[25] J. A. Carrillo, D. Kalise, F. Rossi, and E. Trélat, "Controlling swarms toward flocks and mills," *SIAM Journal on Control and Optimization*, vol. 60, no. 3, pp. 1863–1891, 2022.